

A Novel Approach to the Hydrothermal Synthesis of Anatase Titania Nanoparticles and the Photocatalytic Degradation of Rhodamine B

Murat AKARSU¹, Meltem ASİLTÜRK², Funda SAYILKAN³,
Nadir KİRAZ⁴, Ertuğrul ARPAÇ¹ and Hikmet SAYILKAN^{3*}

¹*Institute für Neue Materialien, D-66123, Saarbrücken, GERMANY*

²*İnönü University, Faculty of Arts and Science, Chemistry Department,
44280, Malatya, TURKEY*

³*İnönü University, Faculty of Education, Department of Science,
44280, Malatya, TURKEY*

e-mail: hsayilkan@inonu.edu.tr

⁴*Akdeniz University, Faculty of Arts and Science, Chemistry Department,
07100, Antalya, TURKEY*

Received 26.01.2006

A novel approach was developed for the synthesis of high-dispersed anatase nano-TiO₂ by a hydrothermal process without solvent at 200 °C in 1 h. It was characterized using XRD, TEM, BET and elemental analysis. Nanoparticle-TiO₂ was used as a photocatalyst by considering complete degradation of Rhodamine B (RB) dye. The photocatalytic reaction parameters such as photocatalyst amount, irradiation time and dye concentration were optimized and it was found that 0.125 wt% catalyst in 30 mg/L of RB aqueous solution is adequate for full degradation of RB in 50 min with 770 W/m² irradiation power. Photocatalytic activity of the nanoparticle-TiO₂ was compared with Degussa P-25 at optimum catalysis conditions determined for the nanoparticle-TiO₂. It was concluded that when compared to Degussa P-25, the nanoparticle-TiO₂ can be repeatedly used with increasing photocatalytic activity. The results revealed that the photodegradation of RB proceeds by pseudo first-order reaction kinetics in which the rate constant of the degradation is 0.132 min⁻¹.

Introduction

One of the major sources of environmental contamination is dyestuff, which mainly comes from the textile and photographic industries¹⁻³. Within the overall category of dyestuffs, Rhodamine B dye (RB), one of the most xanthene dyes, is famous for its good stability as a dye laser material. It has become a common organic pollutant; thus the photodegradation of RB is important with regard to the purification of dye effluents. Photocatalytic degradation of several organic contaminants using large bandgap semiconductor particles (such as TiO₂, ZnO, WO₃) has been studied extensively³⁻⁵. These contaminants present in an

*Corresponding author

aqueous suspension of TiO₂ can be degraded with ultraviolet and visible light⁶⁻⁸. As one of the most popular photocatalysts, TiO₂ particles have long been investigated in environmental purification, and decomposition of organics and dyes in wastewater⁹⁻¹¹. The development of high-dispersed nanocrystallites has been intensively pursued because of their technological and fundamental scientific importance^{12,13}. The high-dispersed TiO₂ powder has an advantage in relation to photocatalytical properties.

TiO₂ exists in 3 polymorphs: anatase, brookite and rutile. Rutile is considered the stable form of titania. Anatase is metastable and amorphous titania precursor is crystallized to anatase in the temperature range 300 to 800 °C. Among these polymorphs, anatase-TiO₂ has attracted more attention for its vital use as pigments¹⁴, gas sensors¹⁵, catalysts^{16,17}, and photocatalysts¹⁸⁻²⁰ in response to its application in environmental problems of pollution control and photovoltaics²¹. The catalytic and other properties of these materials strongly depend on the crystallinity, surface morphology, particle size and preparation methods. The increased surface area of nanosized titania particles may prove beneficial for the decomposition of dyes in aqueous media. TiO₂ nanoparticles in powder have real advantages in relation to photocatalytic activity. In order to produce TiO₂ nanoparticles, different preparation processes have been reported, such as the sol-gel process²², hydrolysis of inorganic salts²³, the ultrasonic technique²⁴, microemulsion or reverse micelles and the hydrothermal process²⁵⁻²⁷. Polar or non-polar different solvents have been used in these processes. In other processes apart from the hydrothermal process a high calcination temperature (above 450 °C) is usually required to form a regular crystal structure. However, in the meantime, the high temperature treatment can decline the surface area and loss of some surface hydroxyl or alkoxide groups on the surface of TiO₂ provides easy dispersion. Thus, in this work the hydrothermal process was selected to synthesize nanosize crystallized TiO₂ at low temperature, which is attractive for the further improvement of the photocatalytic activity of TiO₂ as catalysts. Compared with the other TiO₂ powders, these TiO₂ nanoparticles have several advantages, such as fully pure anatase crystalline form, fine particle size with more uniform distribution and high-dispersion either in polar or non-polar solvent, stronger interfacial adsorption and easy coating on different supporting materials. Moreover, the hydrothermal process with an aqueous solvent as reaction medium is environmentally friendly since the reactions are carried out in a closed system and the contents can be recovered and reused after cooling down to room temperature²⁸.

The objective of this work was to develop a novel approach for the hydrothermal synthesis of nanosized-TiO₂ and to examine the photocatalytic behavior of nanosized-TiO₂ for degradation of Rhodamine B dye. The re-use of the synthesized nanosized-TiO₂ catalyst was compared with Degussa P-25 TiO₂ at the optimum catalysis conditions determined previously for nanoparticle-TiO₂.

Experimental

Materials

Tetrabutylorthotitanate [Ti(OBuⁿ)₄] purchased from Alfa Aesar (Germany) was used as the titanium source for the preparation of TiO₂ photocatalyst. Hydrochloric acid from Merck (Germany) (HCl, 37%) was used as the catalyst for alkoxide hydrolysis. Ti(OBuⁿ)₄ and HCl were used without further purification. Rhodamine B dye (RB), purchased from a local textile factory, was of analytical reagent grade and used without further purification; its chemical formula is presented as

mg/L) was added to nanosol of the anatase TiO₂, containing different amounts of TiO₂, so as to make up 25 mL of 30 mg/L solution in each case. Prior to the irradiation, the nano-TiO₂/RB dye sol was poured into the glass reaction cell, which has 12 separate sample compartments and 1 cover. Then it was kept in the dark for 60 min to ensure sufficient adsorption of the dye. The cell was immediately placed in the Solar Box and irradiation with UV light was immediately started at 770 W/m². The samples were collected at regular intervals (5, 10, 20, 30, 40, 50 and 60 min) and concentration changes of dye solution were measured using a UV/VIS spectrometer at 553 nm (λ_{max}) corresponding to the maximal absorption of dye. It must be noted that the nano-TiO₂ sol/RB solution was also transparent before and after the degradation procedure.

The photodegradation process of RB tended to follow pseudo-first-order reaction kinetics in the presence of the catalyst studied in this article. The regression curve of the natural logarithm of RB concentration versus reaction time was almost a straight line. That is,

$$\ln C_0/C = kt$$

where C is the dye concentration (mg/L) at instant t (min), C₀ is the dye concentration (mg/L) at t = 0 (min), and k is a rate constant (min⁻¹).

Catalyst re-use studies

No filtration or centrifuging was needed for the nanoparticle-TiO₂ sol/RB system after the photocatalysis procedure and before UV-VIS spectrophotometric analysis, since the system was already self-dispersed and transparent, i.e. it did not contain any visible solid particles.

Photocatalytic activity of the nanoparticle-TiO₂ was compared with Degussa P-25 for degradation of RB at optimum catalysis conditions determined for the nano-TiO₂, except that Degussa P-25 TiO₂ particles had to be removed from the system by filtration before UV-VIS spectrophotometric analysis.

The certain amounts of nanoparticle-TiO₂ and Degussa P-25 were used to repetitively degrade freshly prepared 30 mg/L RB solutions. After the first use, only Degussa P-25 was filtered and re-used. Then the so-used catalyst was employed to degrade a new 30 mg/L RB solution at the same conditions applied before. The process was repeated 4 times.

Results and Discussion

Characteristics of the TiO₂ photocatalyst

The crystalline phase of the hydrothermally synthesized TiO₂ sample was analyzed by XRD, and its XRD pattern is shown in Figure 1. When the XRD pattern was compared with PDF# 21-1272 data files it was found that all the sharp peaks observed at 25.39, 38.11, 48.47 and 55.01° 2-Theta values in the XRD pattern are consistent with anatase (101), (004), (200) and (211) spacing^{29,30}. Rutile and brookite phases were not detected.

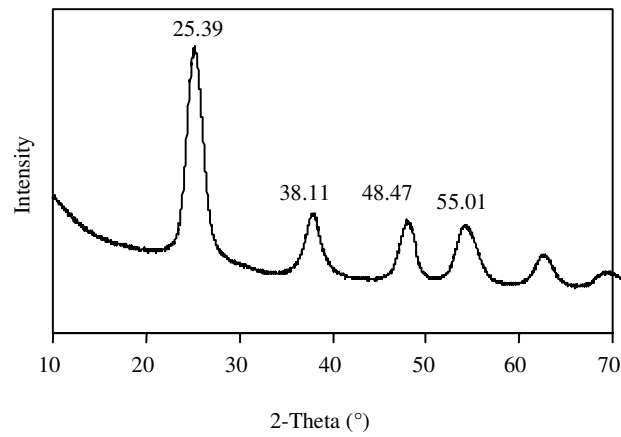


Figure 1. XRD pattern of nano-TiO₂ particle.

TEM photographs of high-dispersed anatase nano-TiO₂ are shown in Figure 2 a-c.

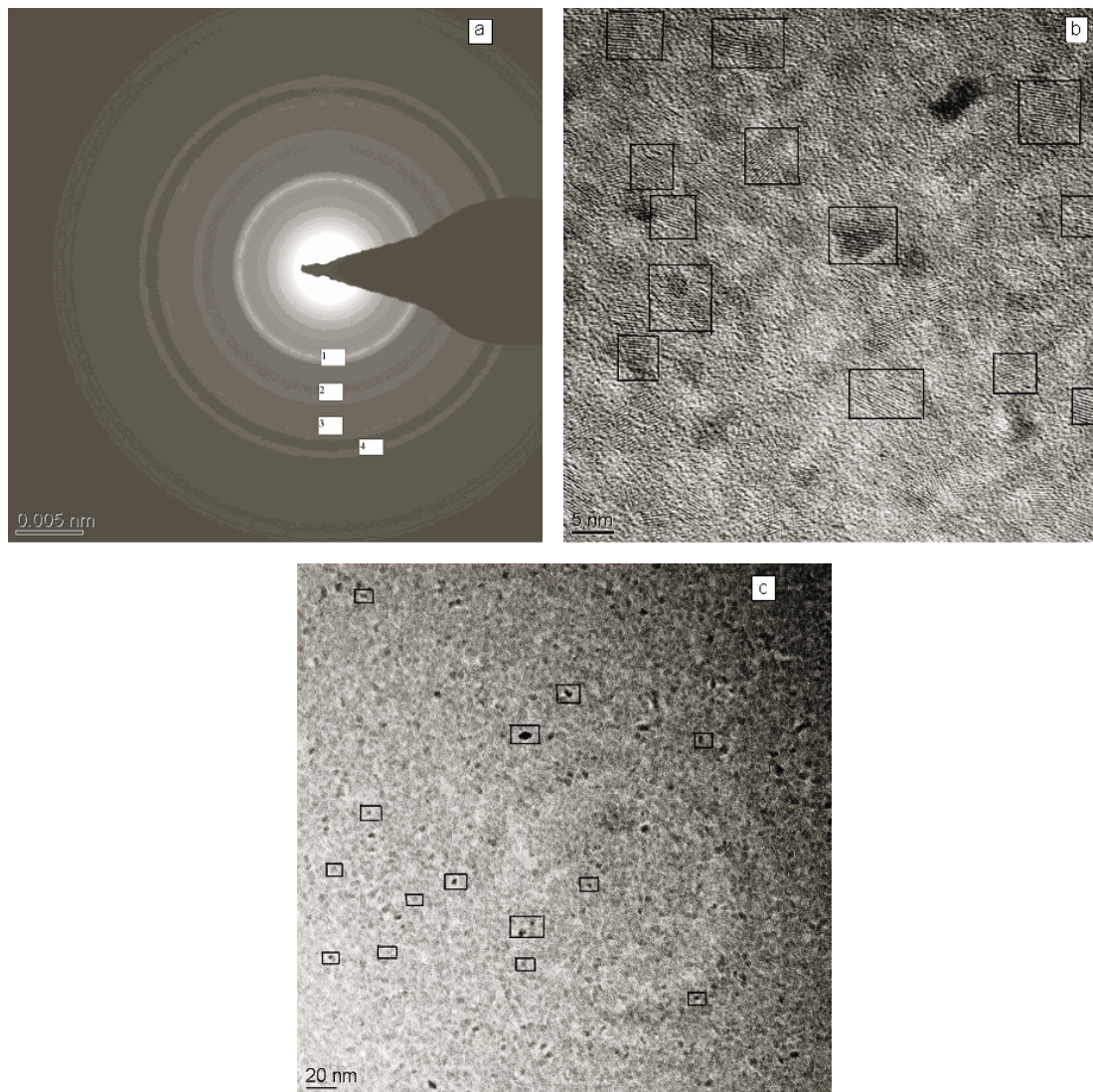


Figure 2. TEM selected area diffraction pattern for synthesized nano-TiO₂ (a, b) and selected particles (c).

In the selected areas of the electron diffraction pattern, the 4 circled areas with spacings of 1, 2, 3 and 4 (Figure 2a) are consistent with anatase (101), (004), (200) and (211) spacings and the corresponding XRD pattern is also shown in Figure 1. In Figure 2b, the circled areas, which generally have regular patterns, show that all particles are anatase crystalline form. The results obtained from XRD and TEM clearly indicate that the synthesized TiO₂ particles are quite close to the anatase crystalline form. The other crystalline forms of TiO₂, rutile and brookite, were not detected in our characterizations. Figure 2c shows some dispersed particles. According to the statistical distribution of these particles, the particle sizes varied between 3 and 7 nm. It can be concluded that the average grain size is 5 nm. The grain size of nano-TiO₂, D, was also estimated from full-width at half-maximum (FWHM) of the diffraction peak of nano-TiO₂ particles after correction of instrumental broadening,

$$D = \lambda / FWHM \cdot \cos \theta$$

where λ is the wavelength of X-ray and θ the Bragg angle. According to this calculation, the particle size was 7.4 nm. It is observed that the particles have different grain sizes obtained from TEM and RXD results.

According to elemental analysis, the TiO₂ contains 10.49% C, 2.52% H, and 2.9% Cl, which means that purity of the TiO₂ is about 84.09%. Some of the physicochemical properties of the synthesized TiO₂ are given in Table 1.

Table 1. Some physicochemical characteristics of the synthesized nanoTiO₂.

Properties	
Crystalline type	Anatase
Grain size	5 nm
TiO ₂ content	84.09%
BET Surface area	40.84 m ² g ⁻¹
Micropore area	39.3095
Micropore volume	0.022 cm ³ g ⁻¹
Adsorption average pore diameter	13.12 Å
Size of micropores	16 Å

The BET surface area and grain size of the nano-TiO₂ are smaller than those of commercial TiO₂ (e.g., P-25 Degussa with 63 m² g⁻¹ specific surface area and 30 nm size and 0.06 ml g⁻¹ pore volume)³⁰. According to the result of the DFT plus method, microporosity dominated and was distributed very little in the range 14-20 Å. The microporosity (percentage of micropores to total pore volume, V_{me}/V_{tot}) was 98.6%. Total pore volume was estimated from nitrogen adsorption at a relative pressure of 0.995. The mesoporosity (percentage of mesopores to total pore volume, V_{me}/V_{tot}) was 1.4%. In general, a decrease in BET surface area with decreasing grain size is not expected. However, the nano-TiO₂ has a micropore structure free from agglomerates, unlike Degussa P-25 particles, which have a mesopore structure. Thus, their properties of N₂ adsorption are different from each other. N₂ adsorption on TiO₂ surface is hindered by butoxide and hydroxide groups bonded to TiO₂, whereas Degussa P-25 does not have these groups. Therefore, even though the grain size is small, the BET surface area of the nano-TiO₂ is also smaller than that of Degussa P-25.

Photocatalytic degradation kinetics

Before examining the photocatalytic activity of the nano-TiO₂ as a catalyst for degradation of RB, adsorption was carried out by keeping 25 mL of sol in its natural pH, containing RB ($C_0 = 30 \text{ mg L}^{-1}$) and Xwt.% TiO₂ (X: 0.125, 0.25, 0.5 and 1, respectively) in the dark at room temperature for 60 min. Approximately 5% of RB was adsorbed on all TiO₂ particles. Thereafter, all TiO₂/RB sols to be subjected to irradiation were soaked for 60 min in the dark.

The degradation of RB was investigated using the hydrothermally synthesized nano-TiO₂ as catalyst under UV irradiation. RB concentrations during degradation realized under different irradiation times and different amounts of nano-TiO₂ in sol are shown in Figure 3.

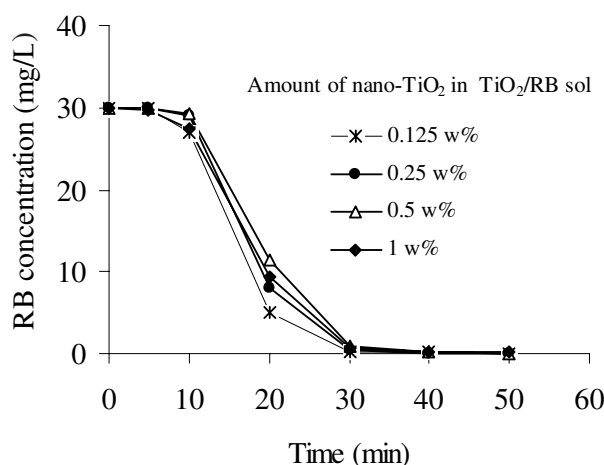


Figure 3. Change in the concentration of RB in the different amount of nano-TiO₂ sol with different irradiation times.

In order to avoid excess catalyst and to ensure total absorption of light photons for efficient photomineralization, usage of the optimum catalyst amount is important. The optimum amount of catalyst is found to be dependent on the initial solute concentration^{31,32}. Shown in Figure 3 is the effect of irradiation time and amount of photocatalyst on RB degradation; 0.125 wt.% TiO₂ in sol easily catalyzes the photooxidation of 30 mg/L RB in 50 min. After this time, the sol was colorless. However, on the other hand, RB/TiO₂ sols, including 0.25, 0.5 and 1 wt.% TiO₂, were cream and yellow. These sols were almost colorless after 70 min irradiation. The slow kinetics of dye degradation after a certain time limit is due to: (a) the difficulty in converting the N-atoms of dye into oxidized nitrogen compounds³³, (b) the slow reaction of short chain aliphatics with OH• radicals, and (c) the short life-time of photocatalyst because of active site deactivation by strong by-product deposition (carbon etc.)³¹.

The color of cream TiO₂/RB sol changed to yellow with increasing initial RB concentration, which indicated that photocatalytic activity of 0.125wt.% nano-TiO₂ was limited to almost 30 mg L⁻¹ RB concentration (Figure 4).

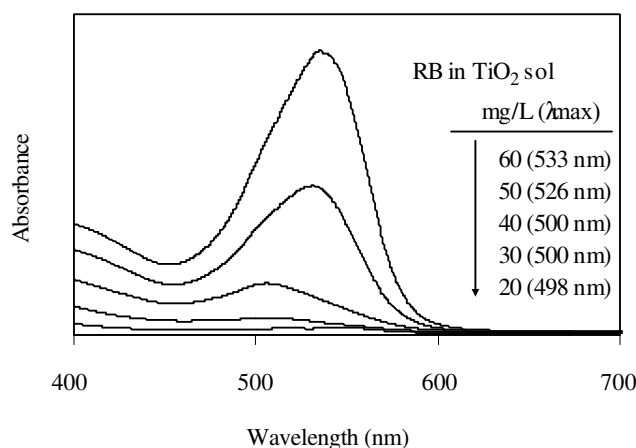


Figure 4. Change in the absorbance spectrum of Rhodamine B in the nano TiO₂ sol (0.125 w%) with initial Rhodamine B concentration (irradiation time: 50 min).

It has been reported that the photodegradation of RB results from both de-ethylation and degradation of RB chromophore structure³⁴. The changes in the absorbance of TiO₂/RB sol were investigated at constant irradiation time of 50 min. As the concentration of RB was decreased to 20 and/or 30 mg/L, maximum absorbance decreased gradually to zero. De-ethylation of RB is the main reaction occurring at the surface, whereas the RB degradation is predominantly a solution bulk process. According to Zhang et al.³⁵, Watanabe et al.³⁶ and Takizawa et al.³⁷, RB is the N,N,N,N'-tetraethylated rhodamine molecule showing λ_{max} at 552 nm. The λ_{max} of RB shifted toward the blue region under UV irradiation (N,N,N,N'-triethylated rhodamine, at 539 nm; N,N-diethylated rhodamine, at 522 nm; N-ethylated rhodamine, at 510 nm and rhodamine at 498 nm). Figure 4 also shows the wavelength shifts of the maximum absorption with different concentrations of RB in 0.125w% TiO₂ sols at 50 min of irradiation.

As can be seen in Figure 4, the maximum absorption shifted from 533 to 498 nm with a decrease in the concentration of RB from 60 to 20 mg/L. The N-de-ethylation products of RB have a light absorption maximum at 500 nm. When RB concentrations are considered, it disappeared rapidly, in 20 and/or 30 mg/L RB solutions, after the N-de-ethylation. From the absorption spectra (Figure 4), no new products or intermediate products causing absorption in the near UV region were observed. The concentration dye has a significant effect on the degradation rates. The higher the concentration is the lower the rate of degradation is. This negative effect can be explained as follows: (a) when the dye concentration increases, the amount of dye adsorbed on the catalyst surface increases and a significant amount of solar light may be absorbed by the dye molecules rather than the catalyst and this may also reduce the catalytic efficiency. b) The rate of degradation relates to the probability of OH[•] radicals, reacting with dye molecules, formation on the catalyst surface. At a high dye concentration, a significant amount of UV may be absorbed by the dye molecules rather than the TiO₂ particles and that reduces the efficiency of the catalytic reaction because the concentrations of OH[•] and O₂^{•-} decrease^{38,39}.

Generally, the logarithmic plots of concentration data give a straight line and its slope is pseudo-first order rate constant. As shown in Figure 5a and b, ln(C₀/C) is linear with the irradiation time, which means that the photodegradation of RB obeyed the rules of a pseudo-first order reaction kinetic. The rate constants of RB photodegradation under the catalysis of different amount of TiO₂, such as 0.125, 0.25, 0.5 and 1 w%

in sol, were 0.1323, 0.1256, 0.1096 and 0.1142 min⁻¹, respectively. The lower amount of catalyst has higher photocatalytic activity than the others.

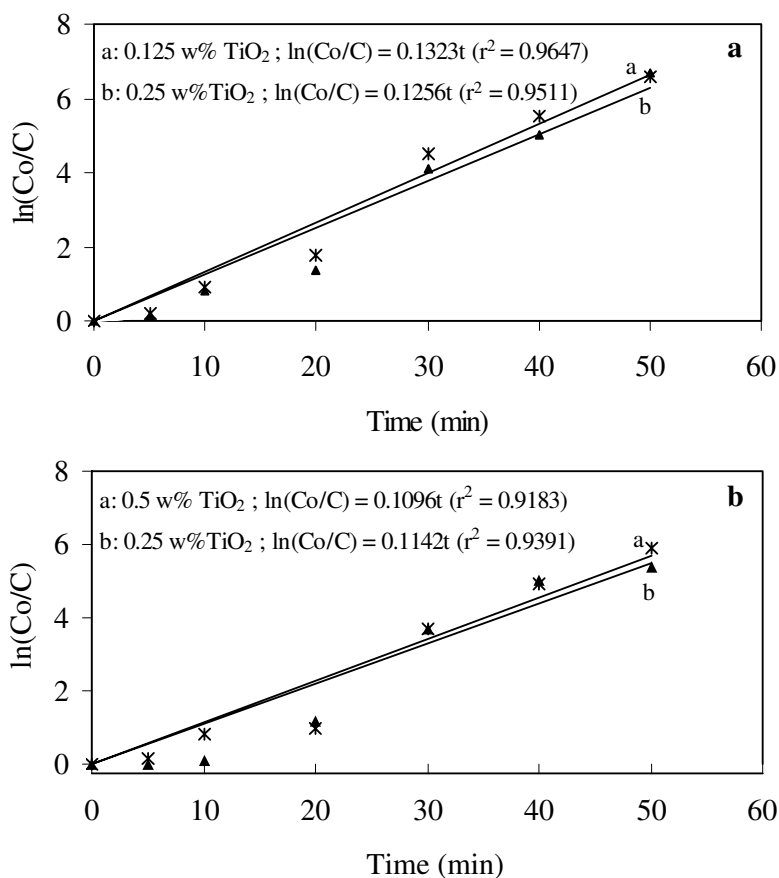


Figure 5. Pseudo-first order photodegradation kinetics of RB.

Catalyst re-use studies

Since the non-removability of the nanoparticle-TiO₂ seems like a disadvantage, re-use of the same sol for degradation of freshly added dye was also investigated. For this purpose, 30 mg/L dye was again and again added to the nano-TiO₂ sol and Degussa P-25 suspension, after complete degradation of the dye was attained.

Degussa P-25 was filtered through a microfilter (0.2 μm) after being used and then it was re-used in the degradation of a new 30 mg/L RB solution in the residual water from the former degradation process at the same optimum photodegradation conditions determined for the nano-TiO₂. The process was repeated 4 times. Table 2 gives the photocatalysis times consumed until complete degradation was observed during the re-use of the catalysts. Too much time was consumed when Degussa P-25 was used. Moreover, after the second use, the photocatalytic activity of Degussa P-25 decreased more, whereas the nano-TiO₂ showed increased activity (i.e. degradation time decreased when the same nano-TiO₂ sol was reused).

Table 2. Comparison of the changes in the degradation times of nano-TiO₂ and Degussa P-25 (the amount of nano-TiO₂ and Degussa P-25 in sol and solution is 0.125w%).

Degradation time, min				
Catalyst	1 st use	2 nd use	3 rd use	4 th use
The nano-TiO ₂	50	40	40	60
Degussa P-25	70	140	170	180

It was observed during the experiments that Degussa P-25 adsorbs more dye than the nano-TiO₂, resulting in a decrease in the degradation rate. This may be due to the high pore volume and pore diameter of the Degussa P-25. Moreover, as the amount of dye adsorbed on the surface of catalyst increases, the active sites may be covered with dye ions, and the formation of OH• radicals decreases. Higher dye adsorption of Degussa P-25 was also observed during repeated usage.

Conclusions

Easily dispersed photocatalytic pure anatase titania (TiO₂) nanoparticles with a 5 nm average grain size in water were successfully synthesized by hydrothermal process without solvent at 200 °C in 1 h. The synthesized nano-TiO₂ particles are fully anatase crystalline form and are highly dispersed in polar and apolar solvent systems since they are amphiphilic. It is a very efficient photocatalyst for complete degradation of higher concentrations of RB in very short irradiation times. Oxidation conditions were determined for the photocatalytic degradation of Rhodamine B. Repeated usage of the high-dispersed catalyst was compared with Degussa P-25 and the synthesized anatase TiO₂ showed higher photocatalytic activity than Degussa P-25, even after the second use. This novel approach was improved in the synthesis of high-dispersed photocatalytic anatase titania (TiO₂) nanocrystals by hydrothermal process and may also be applied to synthesize other oxide composition, such as Zr and Sn, high-dispersed nanoparticles. Furthermore, photocatalytic active thin films based on water or organic solvents may also prepared with these nano-TiO₂ sols.

Acknowledgment

The authors gratefully acknowledge the financial support of Scientific Research Projects Unit (SRPU) at İnönü University, Turkey (SRPU-2004/01).

References

1. A. Fujishima, K. Hashimoto and T. Watanabe, TiO₂ Photocatalysis Fundamentals and Applications, BKC, Inc., Tokyo, 1999.
2. W.C. Tincher, **Text. Chem. Color** **21**, 23 (1989).
3. M.R. Hoffmann, S.T. Martin, W.Y. Choi and D.W. Bahnemann, **Chem. Rev.** **95**, 69 (1995).
4. D. Yu, R. Cai and Z. Liu, **Spectrochim. Acta Part A**: **60**, 1617 (2004).
5. A. Sclafani and L. Palmisano, **Solar Energy Mater. Solar Cells** **51**, 203 (1998).

6. F.L. Zhang, J.C. Zhao and L. Zang et al., **J. Mol.Catal. A: Chem.** **120**, 173 (1997).
7. P. Qu, J. Zhao and T. Shen, **J. Mol. Catal. A: Chem.** **129**, 257 (1998).
8. T.X. Wu, G.M. Liu and J.C. Zhao, **J. Phys. Chem. B** **102**, 5845 (1998).
9. A. Fujishima and K. Honda, **Nature** **238**, 37 (1972).
10. E. Pelizzetti and C. Minero, **Electrochim. Acta** **38**, 47 (1993).
11. T. Hisanaga, K. Harada and K. Tanaka, **J. Photochem. Photobiol. A: Chemistry** **54**, (1990) 113.
12. K.N.P. Kumar, K. Keizer, A.J. Burggraaf and T. Okubo, **Nature** **358**, 48 (1992).
13. C. Wang and J. Ying, **Chem. Mater.** **11**, 3113 (1999).
14. J.G. Balfour, **Technological Applications of Dispersions**, Marcel Dekker, New York, 1994.
15. Y.C. Yeh, T.T. Tseng and D.A. Chang, **J. Am. Ceram. Soc.** **72**, 1472 (1989).
16. C.G. Bond, and S.F. Tahir, **Appl. Catal.** **71**, 1 (1991).
17. P.S. Awati, S.V. Awate, P.P. Shah, V. Ramaswamy, **Catal. Comm.** **4**, 393 (2003).
18. A. Hagfeldt and M. Gratzel, **Chem. Rev.** **95**, 49 (1995).
19. Y.H. Hsien, C.F. Chang, Y.H. Chen, S. Cheng, **Appl. Catal. B: Environmental** **31**, 241 (2001).
20. C. Lizama, J. Freer, J. Baeza and H.D. Mansilla, **Catal. Today** **76**, 235 (2002).
21. N. Serpane, J. Texier, A.V. Emeline, P. Pichat, H. Hidaka and J. Zhao, **J. Photochem. Photobiol. A: Chemistry** **136**, 145 (2000).
22. G. Colon, M.C. Hidalgo and J.A. Navio, **Catal. Today** **76**, 91 (2002).
23. Y. Zhang, G. Xion, N. Yao, W. Yang and X. Fu, **Catal. Today** **68**, 220 (2001).
24. X.M. Wu, L. Wang, Z.C. Tan, G.H. Li and S.S. Qu, **J. Solid State Chem.** **156**, 220 (2001)
25. E. Vigil, J.A. Ayllon, A.M. Peiro and R.R. Clemente, **Langmuir** **17**, 891 (2001).
26. H. Zhang, M. Finnegan and J.F. Banfield, **Nano Letters** **1**, 81 (2001).
27. X. Ju, P. Huang, N. Xu and J. Shi, **J. Membran Sci.** **202**, 63 (2002).
28. G. Demazeau, **J. Mater. Chem.** **9**, 15 (1999).
29. H. Bala, J. Zhao, Y. Jiang, X. Ding, Y. Tian, K. Yu and Z. Wang, **Mater. Lett.** **59**, 1937 (2005).
30. I. Kartini, P. Meredith, J.C. Diniz Da Costa and G.Q. Lu, **J. Sol-Gel Sci. Technol.** **31**, 185 (2004).
31. I.K. Konstantinou and T.A. Albanis, **Applied Catalysis B: Environmental** **49**, 1 (2004).
32. J.M. Hermann, **Catal. Today** **53**, 115(1999).
33. J. Bandara, V. Nadtochenko, J. Kiwi and C. Pulgarin, **Water Sci. Technol.** **35**, 87 (1997).
34. H.M. Sung-Suh, J.R. Choi, H.J. Hah, S.M. Koo and Y.C. Bae, **J. Photochem. Photobiol.A: Chem.** **163**, 37 (2004).
35. Y. Zhang, H. Xu, Y. Xu, H. Zhang and Y. Wang, **J. Photochem. Photobiol.A: Chem.** **170**, (2005) 279.
36. T. Watanabe, T. Takizawa and K. Honda, **J. Phys. Chem.** **81**, 1845 (1977).
37. T. Takizawa, T. Watanabe and K. Honda, **J. Phys. Chem.** **82**, 1391 (1978).
38. C.M. So, M.Y. Cheng, J.C. Yu and P.K. Wong, **Chemosphere** **46**, 905 (2002).
39. L.B. Reutergerth and M. Iangphasuk, **Chemosphere** **35**, 585 (1997).